

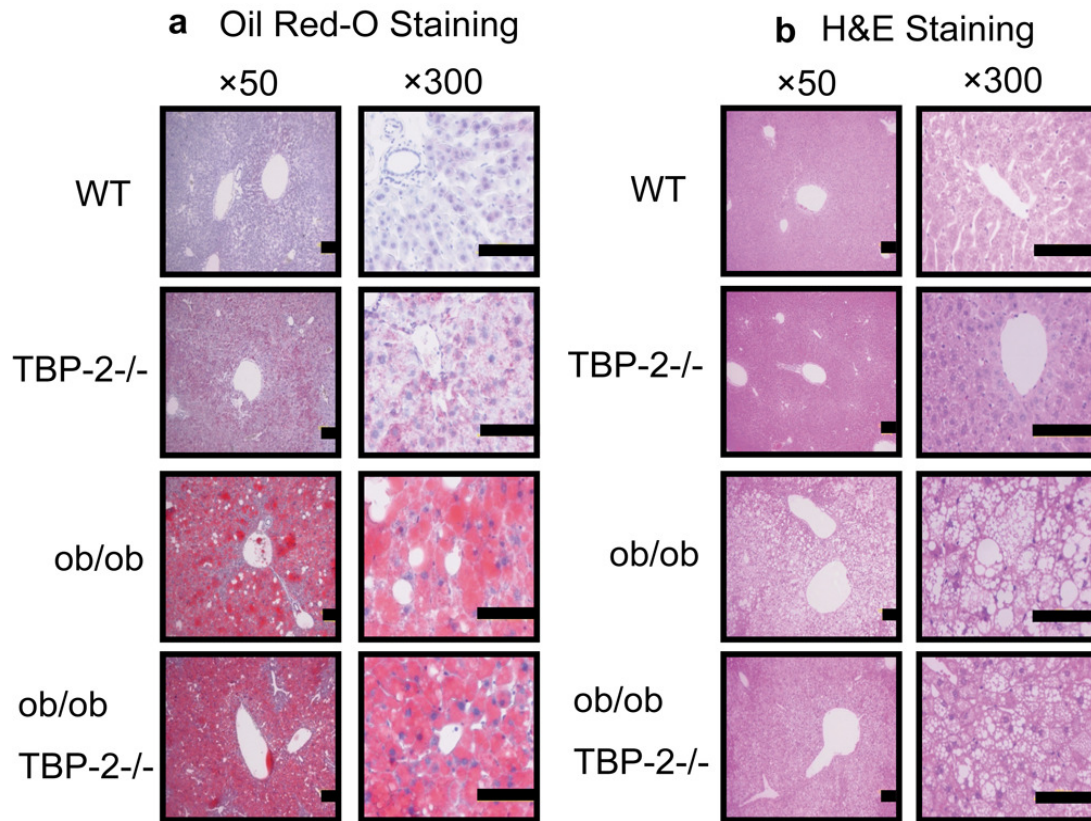
Supplementary Information

**Disruption of TBP-2 ameliorates insulin sensitivity and
secretion without affecting obesity**

Eiji Yoshihara, Shimpei Fujimoto, Nobuya Inagaki, Katsuya Okawa, So Masaki,

Junji Yodoi & Hiroshi Masutani

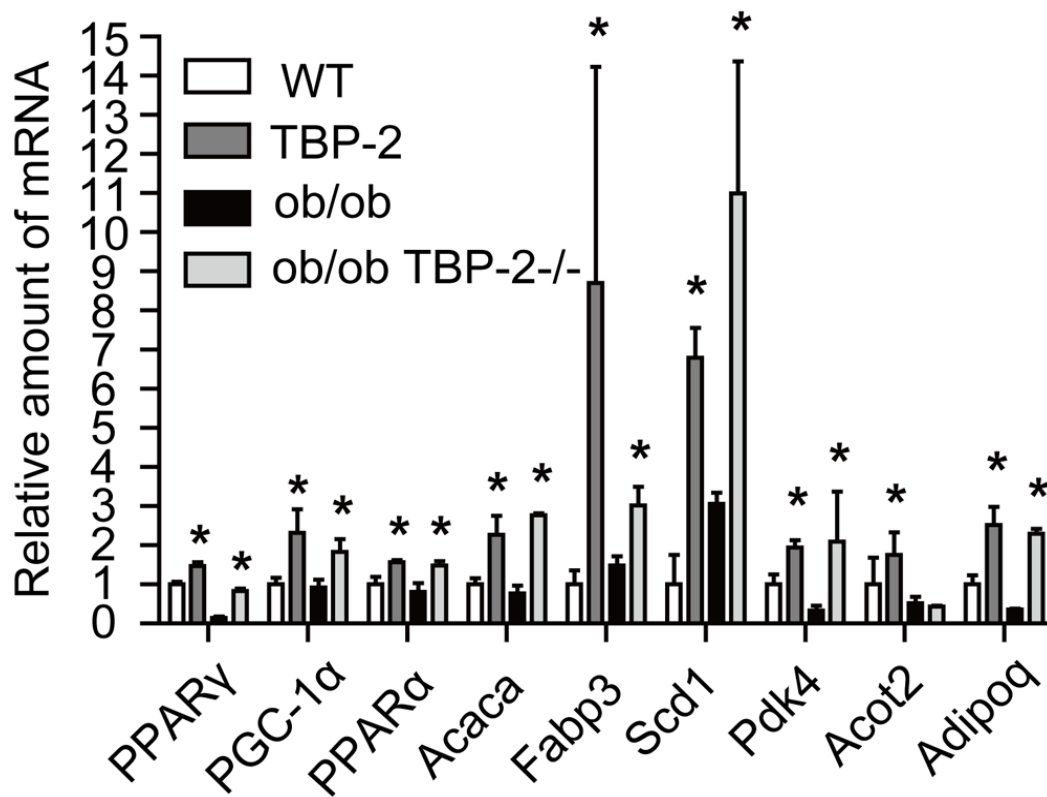
Supplementary Figures



Supplementary Figure. S1. Liver steatosis occurred in *ob/ob* and *ob/ob·TBP-2^{-/-}*

mice

Light microscopic view of Oil-Red-O stained (a) and H&E stained (b) sections of liver from WT, *TBP-2^{-/-}*, *ob/ob*, *ob/ob·TBP-2^{-/-}* mice. Magnification, x50 and x300. Scale bar is 100 μm.

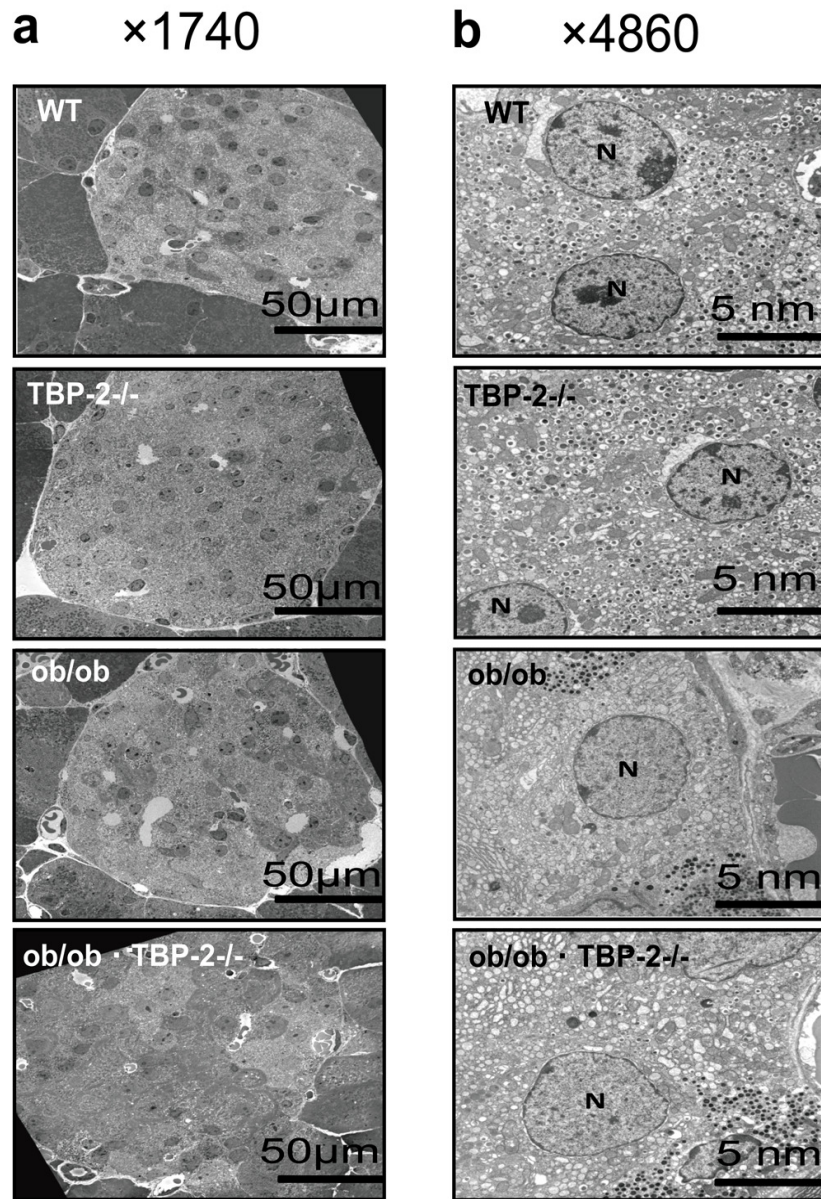


Supplementary Figure. S2. PPAR signaling target genes are upregulated by TBP-2 deficiency in skeletal muscle.

Real-time PCR analysis of the expression of PPAR signaling target genes from the skeletal muscle of 10 weeks of age WT, TBP-2^{-/-}, ob/ob and ob/ob·TBP-2^{-/-} mice.

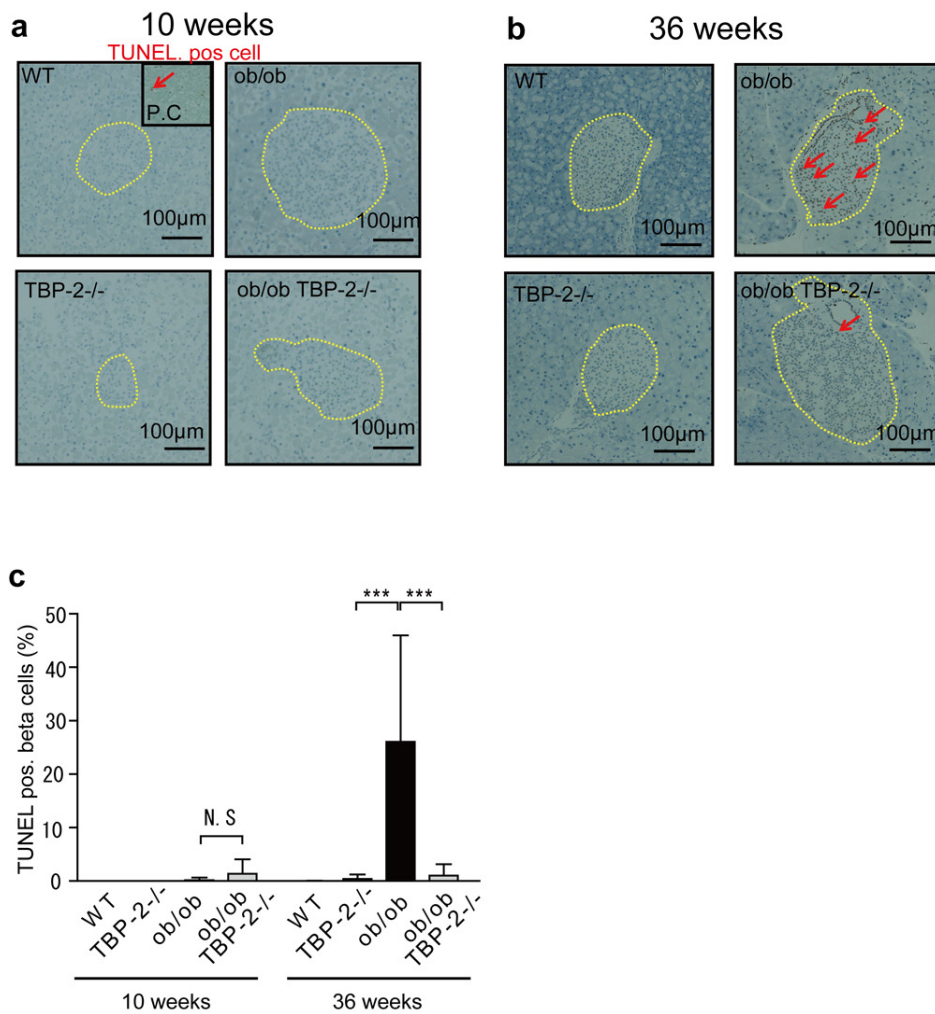
Asterisk indicates * $P < 0.05$; WT vs TBP-2^{-/-}, WT vs ob/ob, ob/ob vs ob/ob·TBP-2^{-/-}.

Data are presented as mean \pm s.d, n=3, * $P < 0.05$, ** $P < 0.01$, *** $P < 0.001$, versus control (*t*-test).



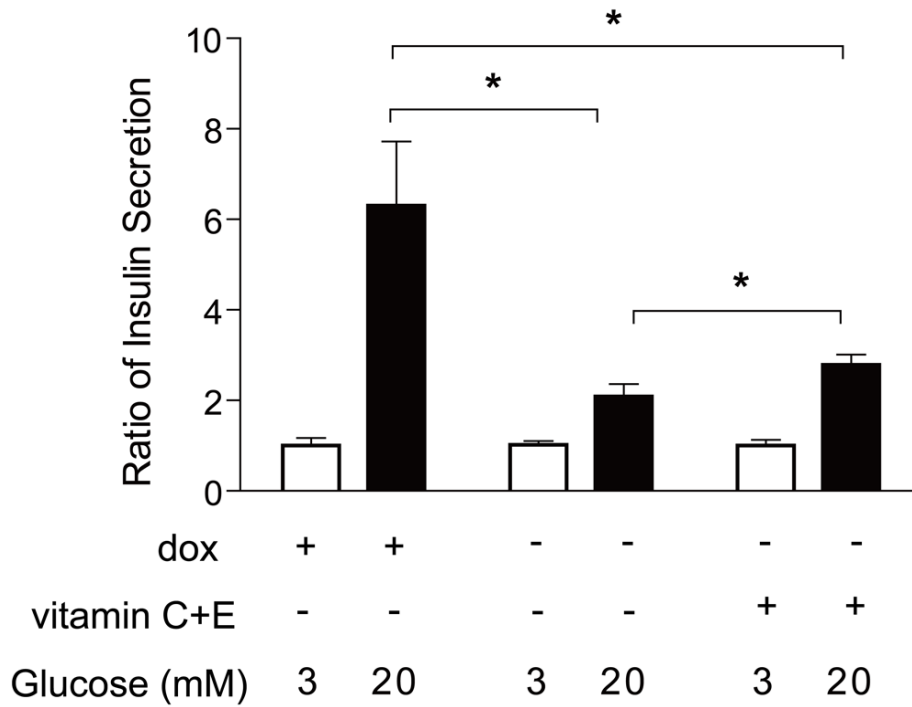
Supplementary Figure. S3. Electron microscopic analyses of pancreatic islets.

(a) Electron microscopic images of islet sections (×1740; scale bar 50 μm). Whole islets are shown. (b) Electron microscopic images of islet sections (×4860; scale bar 5 μm). Magnified areas of an individual β-cell nucleus (labeled with “N”).



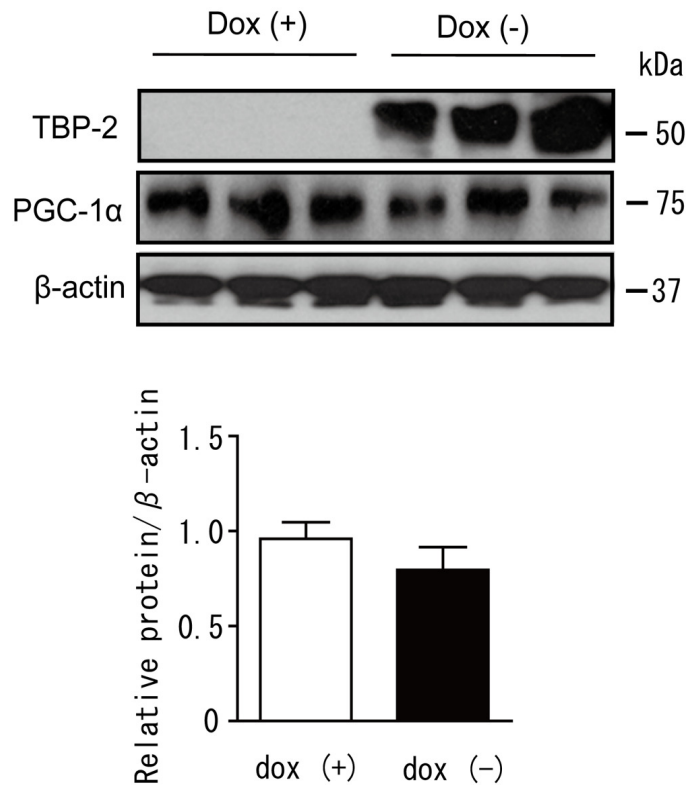
Supplementary Figure S4. TBP-2 deficiency protects against obesity-induced β -cell apoptosis in old mice but not young mice.

Representative pancreas sections of WT, TBP-2^{-/-}, ob/ob and ob/ob·TBP-2^{-/-} mice at 10 weeks (young) (a) and at 36 weeks (old) (b) of age. β -cell apoptosis rate was assessed by TUNEL staining. (c). P.C. in (a) means positive control. ~85 islets and ~19,000 cells were analyzed per group. Data are presented as mean \pm s.d, n=3, *** P < 0.001, versus control (t -test).



Supplementary Figure S5. ROS scavengers did not significantly change the effect of TBP-2 overexpression in GSIS.

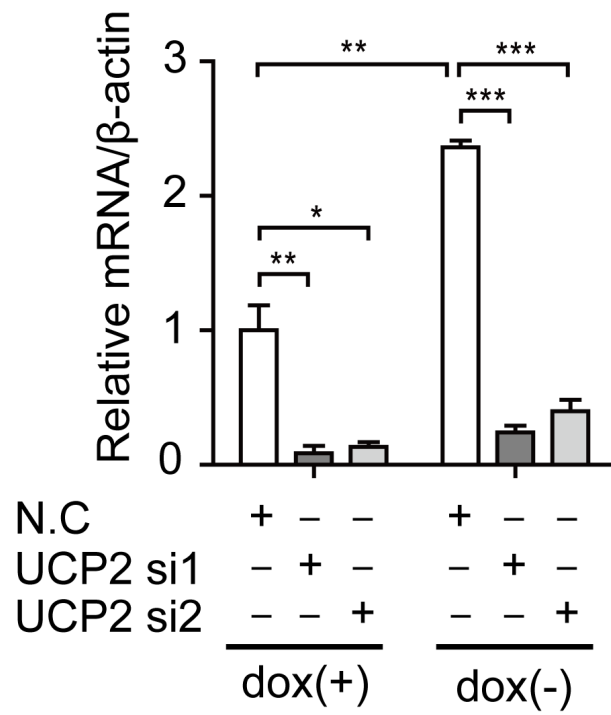
After preincubation with 3 mM glucose with or without reactive oxygen species (ROS) scavengers (200 μ M ascorbate plus 100 μ M α -tocopherol, vitamin C+ vitamin E), INS-1 cells were cultured for 30 min at 3 mM glucose or 20 mM glucose in the presence or absence of ROS scavengers. Data are presented as mean \pm s.d, n=3, * P < 0.05, versus control (t -test).



Supplementary Figure. S6. Dox-off induced TBP-2 overexpression does not affect PGC-1α expression.

Immuno blotting (IB) analyses to determine PGC-1α expression in dox-off TBP-2 overexpression in INS-1 cells (upper). Densitometric quantification of the PGC-1α/β-actin ratio in dox-off induced TBP-2 overexpression in INS-1 cells (lower).

Data are presented as mean ± s.d, n=3.



Supplementary Figure S7. Real Time RT-PCR analysis.

Quantification of UCP-2 mRNA level to confirm UCP-2 knockdown in INS-1 cells. Data

are presented as mean \pm s.d, n=3.

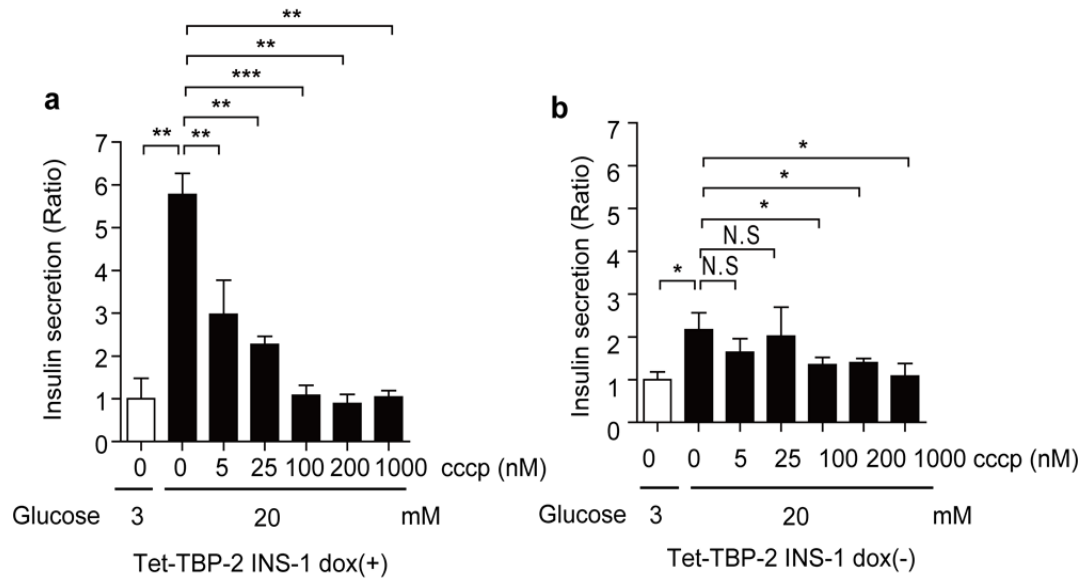


Figure. S8. The mitochondrial uncoupling reagent cccp reversed the ameliorative effects of TBP-2 deficiency on GSIS in ob/ob islets.

(a) Suppression of insulin secretion by cccp treatment for 30 min in dox (+) tet-TBP-2 INS-1 cells. (b) Suppression of insulin secretion by cccp treatment for 30 min in dox (-) tet-TBP-2 INS-1 cells.

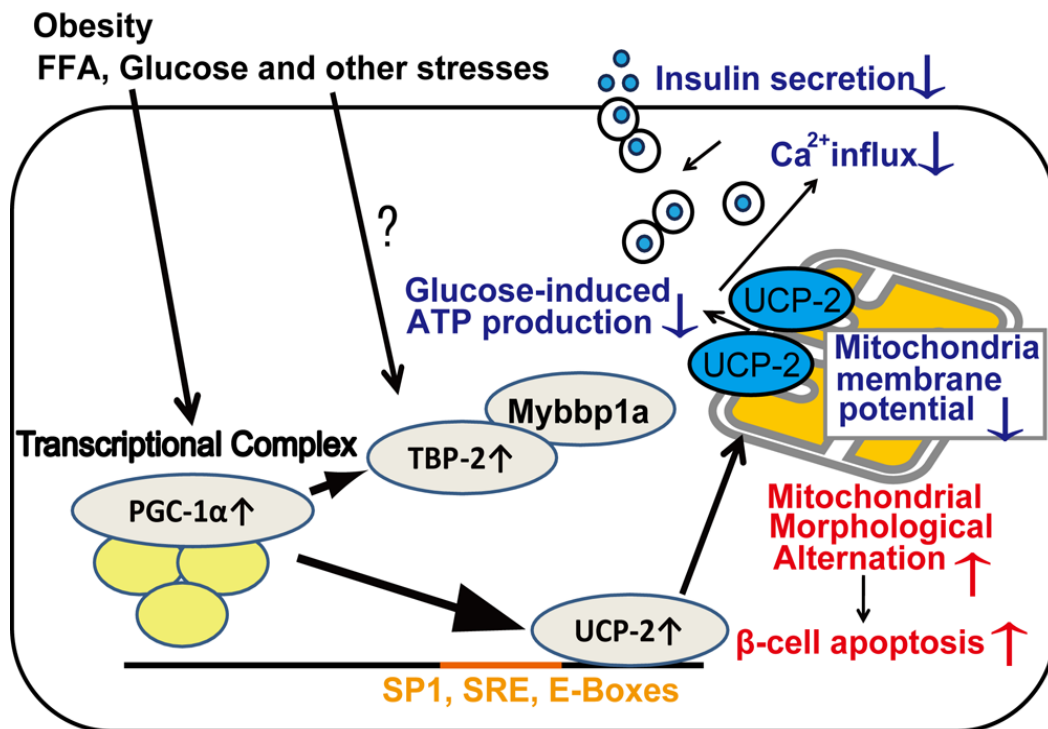


Figure. S9. A model for metabolic function of TBP-2 and the role in diabetes.

Negative regulation of insulin secretion by TBP-2 through UCP-2 expression. TBP-2 is induced in a wide variety of conditions, including obesity, and TBP-2 upregulates UCP-2 expression. UCP-2 suppresses mitochondrial membrane potential, ATP production, Ca²⁺ influx and insulin secretion in pancreatic β-cells.

Supplementary Table

Supplementary Table S1 Serum physiological parameters at 15 weeks of age.

Measurement	Unit	WT	TBP-2-/-	ob/ob	ob/ob	<i>P</i>	<i>P</i>
		N=9	N=9	N=10	TBP-2-/- N=12	value *	value **
AST(GOT)	IU/L	78.6±18.6	130.4±97.3	205.8±104.4	184.7±58.2	0.067	0.277
ALT(GPT)	IU/L	15.2±4.4	31.3±38.9	150.9±91.7	131.75±62.1	0.118	0.283
ALP	IU/L	304.4±66.7	320.5±71.1	582.1±239.9	493.7±138.4	0.309	0.146
LDH	IU/L	457.9±107.5	366.8±96.8	481.3±310.9	489.8±199.9	0.034	0.469
Total Cholesterol	mg/dL	70.6±14.4	80.1±26.1	169.0±48.4	174.9±52.6	0.173	0.435
Triglycerides	mg/dL	38.6±23.0	39.4±26.1	45.6±21.0	50.8±24.7	0.470	0.301
Free Fatty Acids	mEq/L	1.11±0.37	2.25±1.02	1.99±0.51	2.46±0.75	0.003	0.049
Sodium	mEq/L	152.9±1.4	152.8±2.0	154.9±2.6	158.3±5.6	0.457	0.050
Chloride	mEq/L	113.0±2.2	111.9±2.2	108.6±4.7	111.5±7.4	0.147	0.154
Potassium	mEq/L	5.20±0.91	5.98±0.75	4.97±0.62	5.76±0.54	0.029	0.003
Calcium	mg/dL	8.59±0.53	8.96±0.59	9.96±0.61	9.87±0.76	0.084	0.372
BUN	mg/dL	27.2±5.8	20.6±7.6	28.7±5.3	31.1±6.4	0.024	0.171
Creatinine	mg/dL	0.11±0.01	0.09±0.02	0.09±0.01	0.08±0.03	0.006	0.330
Ketone Body	μmol/L	170.7±96.3	692.2±473.4	256.2±140.3	347.2±100.2	0.002	0.045
Phospholipid	mg/dL	138.0±22.6	140.2±44.4	310.5±71.0	322.3±66.5	0.474	0.386

**P* value WT vs TBP-2-/-; ** *P* value ob/ob vs ob/ob TBP-2-/-; *P*<0.05 is shown in red

The unit abbreviations are shown below.

IU/L: International Unit/ Liter

mEq/L: mili-Equivalent/ Liter

mg/dL: milligram/deciliter

μmol/L: micro-mol/ Liter

Supplementary Table S2

Microarray analyses in skeletal muscle of each genotyped mouse. Insulin signaling related genes were picked up.

UniGene	WT	TBP-2-/-	ob/ob	ob/ob TBP-2-/-	Gene Symbol
Mm.268521	-0.06381273	0.46117544	-0.60882044	0.06381273	Igf1
Mm.294740	-0.9296303	-0.035288334	0.035288334	0.34242058	Igf2bp2
Mm.233799	-0.7044463	0.016175747	-0.016175747	0.22599173	Igfbp4
Mm.233799	-0.78458285	-0.07599282	0.07599282	0.35680652	Igfbp4
Mm.4952	-0.041382313	0.85098448	-0.7441888	0.413823133	Irs1
Mm.259333	-0.46301222	-0.10926485	0.5443597	0.10926485	Pik3r1
Mm.244960	-0.39844537	1.4427922	-0.28484654	0.8454654	Pik3r5
Mm.313977	-0.5254824	0.07137942	-0.07137942	0.21943831	Pip5k2
Mm.39424	-0.6025313	-0.048639536	0.048639536	0.6824105	Shc2
Mm.7601	-0.25032377	0.25032377	-0.54563856	0.53975725	Sla

Normalized intensity values (Log scale) are shown.

Upregulation is shown in red and downregulation is shown in blue.

TBP-2-/- compared with WT, ob/ob compared with WT, ob/ob·TBP-2-/- compared with ob/ob.

Supplementary Table S3

TBP-2/Txnip-bound proteins identified by mass spectrometry.

Fig. 7b Number	Gene Name
1	Cytoplasmic dynein 1 heavy chain
2	Translocated promoter region, PREDICTED: multiple ankyrin repeats, single H-domain homolog
3	Spectrin alpha, Spectrin beta
4	GCN111 protein, Spectrin beta
5	Myb-binding protein 1A
6	Myb-binding protein 1A
7	Myb-binding protein 1A, General transcription factor II-I
8	MutS homolog 2, staphylococcal nuclease domain-containing protein 1
9	NoO/p54nrb homolog
10	78kDa glucose-regulated protein, Heat shock cognate 71kDa protein
11	DEAD (Asp-Glu-Ala-Asp) box polypeptide 5, Ribophorin I
12	TBP-2, Tubulin beta, Tubulin alpha, Heterogenous nuclear ribonucleoproteinI
13	Tubulin beta, Tubulin alpha, ATP synthetase beta

Supplementary Table S4

Sequence of primers used for quantitative or semiquantitative RT-PCR analyses.

Gene	Sense Primer	Antisense primer
M TBP-2/TXNIP	5'-GTGATGGATCTAGTGGATGTC-3'	5'-TCACTGCACGTTGTTG-3'
M β -ACTIN	5'-ATGGATGACGATATCGCTGCGCT-3'	5'-TAGAAGCACTTGCCGTGCACGAT-3'
M UCP-2	5'-GCCACTTCACTTCTGCCTTC-3'	5'-GAAGGCATGGCCCCTTGTA-3'
M COXI	5'-ACTATACTACTACTAACAGACCG-3'	5'-GGTTCTTTTTTTCCGGGAGTA-3'
M Cyclophilin	5'-ACACGCCATAATGGCACTGG-3'	5'-CAGTCTTGGCAGTGCAGAT-3'
M IGF-1	5'-ACTCACCACCCTGTGACCTC-3'	5'-CTCCTGGAAACCCAGAACAA-3'
M IGF2BP2	5'-GCAAAGAAGGCAGAAACCTG-3'	5'-TTAGCCCTGGGATCAGATTG-3'
M IGFBP4	5'-CCCTATGCTCTGGGGTTGTA-3'	5'-GGCTTATCCTGTAGGGCACA-3'
M IRS-1	5'-CCAGCCTGGCTATTTAGCTG-3'	5'-CCCAACTCAACTCCACCACT-3'
M IRS-2	5'-TAGCCACAGGAGCAACACAC-3'	5'-CAGGCGTGGTTAGGGAGTAA-3'
M Pik3r1	5'-GGAGGTGAAGCTGAGAGTGG-3'	5'-TGTCCATCTGTCCTCCATCA-3'
M Pik3r5	5'-CAGTCCCTGAAGGCAGACTC-3'	5'-CAGTCCCTGAAGGCAGACTC-3'
M AKT3	5'-GAAACTGGCCACTTCTGCTC-3'	5'-ACTGAGGTGTGGTGGAGACC-3'
M PPAR γ	5'-CTGTGAGACCAACAGCCTGA-3'	5'-AATGCGAGTGGTCTTCCATC-3'
M PGC-1 α	5'-ATGTGTGCGCTTCTTGCTCT-3'	5'-ATCTACTGCCTGGGGACCTT-3'
M PPAR α	5'-GAGGGTTGAGCTCAGTCAGG-3'	5'-GGTCACCTACGAGTGGCATT-3'
M ACACA	5'-GCCTCTTCTGACAAACGAG-3'	5'-TGACTGCCGAAACATCTCTG-3'
M FABP3	5'-GACGAGGTGACAGCAGATGA-3'	5'-TGCCATGAGTGAGAGTCAGG-3'
M SCD1	5'-CGAGGGTTGGTTGTTGATCT-3'	5'-GCCCATGTCTCTGGTGTTTT-3'
M PDK4	5'-GCCTTGGGAGAAATGTGTGT-3'	5'-GAAGGCCTGGCTTTTTGAG-3'
M ACOT2	5'-CCAAGTGCTGGGAGTAAAGC-3'	5'-TTTGTCGTCTTACGGCACTG-3'
M ADIPOQ	5'-GTTGCAAGCTCTCCTGTTCC-3'	5'-TCTCCAGGAGTGCCATCTCT-3'
R TBP-2/Txnip	5'-CTGATGGAGGCACAGTGAGA-3'	5'-CTCGGGTGGAGTGCTTAGAG-3'
R UCP-2	5'-GCATTGGCCTCTACGACTCT-3'	5'-CTGGAAGCGGACCTTTACC-3'
R β -ACTIN	5'-CACGATGGAGGGGCCGACTCAT-3'	5'-AAAGACCTCTATGCCAACACAGT-3'
H TBP-2/TXNIP	5'-GCCACACTTACCTTGCCAAT-3'	5'-GGAGGAGCTTCTGGGGTATC-3'

M = mouse ; R = rat ; H = human.

Supplementary methods

Body weight, food intake, water intake, blood glucose, serum insulin and urine glucose

Mice were individually housed and maintained from the time of weaning on regular chow. Body weights, food intake, water intake, blood glucose and blood insulin were measured weekly at the same time of day, from 4 weeks - 15 weeks of age. Blood glucose values were determined by Glucose PILOT (Aventir Biotech, LLC) and blood insulin values were determined by Levis Insulin KIT (Shibayagi). Urine glucose was measured in urine specimens (TERUMO).

Serum physiological parameters in mice aged 15 weeks

Blood was collected in the absence of anticoagulants from the retro-orbital or tail vein. Serum physiological parameters were measured by FALCO biosystems.

Body fat composition analyses

The adiposity of mice was examined radiographically using CT (LaTheta, ALOKA) according to the manufacture's protocol. We performed CT scanning at 5-mm intervals from the diagram to the bottom of the abdominal cavity.

Histological analyses

Immunostaining of insulin was performed by Falco Biosystems (JAPAN). Islets mass was measured by Image J.

Fatty-acid solution (palmitate)

Stock solutions were prepared as follows: palmitic acid (Sigma) was dissolved in ethanol:H₂O (1:1, vol:vol) at 50 ° C at a final concentration of 150 mM. Aliquots of stock solutions were complexed with fatty-acid free BSA (10 % solution in H₂O, Sigma) by stirring for 1h at 37 ° C and then diluted in culture medium. The final molar ratio of fatty acid:BSA was 5:1. The final ethanol concentration was ≤ 0.33 % (vol:vol). All control conditions included a solution of vehicle (ethanol: H₂O) mixed with fatty-acid free BSA at the same concentration as the palmitate solution.

Detection of apoptosis by annexin V-FITC staining

Before assays, cells were cultured with or without doxycycline for 2 days. Annexin V-FITC staining was performed with various time durations of high glucose (25 mM glucose) stimulation. The cells were washed with PBS, resuspended in 500 μ l of binding buffer (10 mM HEPES NaOH, pH 7.4, 150 mM NaCl, pH 7.4, 150 mM NaCl, 5 mM KCl, 1 mM MgCl₂, and 1.8 mM CaCl₂), incubated for 15 min with 5 μ l of 50 μ g/ml Annexin-V (BD Pharmingen, USA) and detected by a BD FACS Canto II flow cytometry system (BD Bioscience). Data were analyzed and plotted using FlowJo software (Treestar).

Immunoblotting

5 min (for heart and liver) or 8 min (for skeletal muscle) after intraperitoneal insulin injection (1U/kg), tissues of mouse heart, skeletal muscle and liver or cultured INS-1 cells were lysed in a lysis buffer containing 50 mM Tris (pH 7.5), 150 mM NaCl, 10 mM EDTA, 1 % NP40, 1 % Na-deoxycholate, 0.1% SDS, protease inhibitors (Roche) and phosphatase inhibitors (Roche). Total protein lysates (10-30 μ g) were analyzed by

SDS-PAGE. Proteins were transferred to PVDF membranes and detected by antibodies against pAKT (1 µg/ml, Cell Signaling), AKT (1 µg/ml, Cell Signaling), pFoxO1 (1 µg/ml, Cell Signaling), IRS-1 (1µg/ml, Cell Signaling), UCP-2 (1 µg/ml, Santa Cruz), TBP-2 (JY2, 1 µg/ml, MBL), PGC-1α (1 µg/ml, Santa Cruz) and β-actin (1 µg/ml, Sigma). Membranes were stripped in Re-Blot Plus Mild Solution (Chemicon) and reprobed with the corresponding antibodies.

Mitochondria isolation

Mitochondria isolation from cultured cell lines was performed using a Mitochondria Isolation Kit for Tissues and Cultured cells (BioChain Institute, Inc.), following their protocols.

Electron microscopy

For ultrastructural examinations, pancreas samples were cut into 1 mm square sections and sections were fixed for 36 h at 4 °C in mol/l in 0.1 mM sodium phosphate buffer (pH7.4) containing a 2 % paraformaldehyde and 2 % glutaraldehyde. The following methods were performed by Tokai Denshikenbikyousei. The tissue pieces were subsequently washed and dehydrated using graded acetone, and embedded in Epon-Araldite. The ultra thin sections were prepared on an ultra microtome. The sectioned tissues were then stained with 1 % toluidine blue borax solution, mounted on copper grids, and double-stained with uranyl acetate. The grids were examined in a JEM 100 CX-II electron microscope.

Histological analyses

Hematoxylin and eosin (HE) staining, Oil-Red-O staining and TUNEL stain analyses were performed by Falco Biosystems (JAPAN).

Cell culture of primary mouse embryonic fibroblasts.

Primary mouse embryonic fibroblasts (MEFs) were derived from 13.5-day-old embryos from TBP-2^{+/-} mice and then the MEFs were genotyped to obtain TBP-2^{-/-} and TBP-2^{+/+} MEFs. TBP-2 mRNA expression was confirmed by semi quantitative RT-PCR analysis. Primer sequences are listed in Supplementary Table S4. Cells were maintained in DMEM with 10% FCS, 1% penicillin and 0.5% L-glutamine.

Glucokinase and hexokinase assay

Glucokinase (GK) activity was measured by a fluorometric assay according to methods previously described². After INS-1 (tet-system) cells with or without doxycycline for 48 h were preincubated with KRBB medium with 2.8 mM glucose, 2×10^5 cells were homogenized with 250 μ l of solution containing 20 mM KH₂PO₄, 100 mM KCl, 1 mM MgCl₂, 1 mM EDTA, 5% glycerol, and 1 mM DTT (pH7 by KOH), and the supernatant (INS-1 extract) was obtained from the homogenate by centrifugation (10000g, 15 min). The glucose phosphorylation rate was estimated as the increase in NADH through the following reaction: glucose-6-phosphate + NAD \rightarrow 6-phosphoglucono- δ -lactone + NADH by NAD dependent G6PDH. The enzyme reaction was performed using 25 μ l of INS-1 extract in 160 μ l of a solution consisting of 50 mM HEPES (pH 7.4 by NaOH), 100 mM U/ml G6PDH supplemented with two concentrations (50 mM for glucokinase and 0.5 mM for hexokinase) of glucose at 37 °C for 1 h. The reaction was stopped by adding

290 μ l stop of solution (300 mM Na_2HPO_4 , 0.46 mM SDS, pH8.0). NADH concentration was measured by fluorometry (Shimazu RF5000) at excitation and emission of 340 nm and 450 nm, respectively. Blanks in the absence of ATP were incubated in a parallel experiment. Glucokinase activity (Fig. 5g) was calculated, subtracting hexokinase activity (data not shown) measured at 0.5 mM glucose from the activity measured at 50 mM glucose.

Microarray Analyses

Total RNA was extracted from the skeletal muscle of Wild type, TBP-2^{-/-}, ob/ob and ob/ob.TBP-2^{-/-} mice using an RNeasy Fibrous Tissue Mini Kit (Qiagen). Microarray analyses using a Whole Mouse Genome array (Agilent Technologies) were done according to the manufacture's protocols. Data were analyzed by GeneSpring GX software for data mining. Briefly, per-chip normalizations were set to the 75th percentile, and per-gene normalizations to the median and specific samples. To explore the candidates for TBP-2 targets in skeletal muscle, genes assigned as absent were eliminated from the dataset and the genes that showed an expression difference of more than twice that of the WT were picked up. Furthermore, the combination analyses by Go ontology, pathway analyses and cluster analyses were performed. The microarray data have been deposited in the NCBI's Gene Expression Omnibus (GEO) (<http://ncbi.nih.gov/geo/>) and accessible through GEO Series accession number (GSE24851).

Preparation of TBP-2/Txnip-immobilized beads.

Expression plasmids for His-tagged TBP-2 were introduced into competent *Escherichia coli* cells, and the transformed cells were cultured for 12 h [optical density at 650 nm

(OD₆₅₀) = 0.5] in Terrific Broth (Invitrogen). The cells were harvested after incubation with 1 mM isopropyl-beta-D-thiogalactopyranoside (IPTG) for 2 h, and the TBP-2 protein was purified with Ni-chelating magnetic beads (Promega), according to the manufacture's instructions. After PD-10 column chromatography, the purification product of TBP-2 was verified by sodium dodecyl sulfate-polyacryl amide gel electrophoresis (SDS-PAGE). Tosyl (p-toluene sulfonyl)-activated magnetic nano beads (TG-beads) were supplied from Tamagawa Seiki, and 2 mg of beads were mixed with 40 µg of purified His-tagged TBP-2 in the immobilized buffer (10mM HEPES-NaOH [pH 7.9], 10 % glycerol, 50 mM KCl, 1 mM EDTA) at 4 °C for 24 h. The remaining active esters were blocked by incubation with 1 M Tris-HCl [pH 8.0] at 4 °C for 24 h. The resulting beads (TBP-2 protein-immobilized beads) were stored at 4 °C.

Affinity purification with TBP-2 protein-immobilized beads.

INS-1 cells were stimulated by 20 mM glucose containing RPMI cultured medium for 24 h before harvest. Nuclear extract from INS-1 cells were prepared using a Nuclear Extraction Kit (Active Motif). The nuclear extract was incubated with TBP-2 protein-immobilized beads or control beads for 4 h at 4 °C, then washed three times with binding buffer (10 mM HEPES-NaOH [pH 7.9], 10 % glycerol, 100 mM KCl, 1 mM EDTA, 0.1 % NP-40, 1 mM DTT, 0.5 mM PMSF) and once with high-salt buffer (10 mM HEPES-NaOH [pH7.9], 10 % glycerol, 1 M KCl, 1 mM EDTA, 0.1 % NP-40, 1 mM DTT, 0.5 mM PMSF). The bound proteins were eluted with Laemmli sample buffer (Bio-Rad Laboratories) subjected to SDS-PAGE and silver staining by silver stain plus Kit (Bio-Rad Laboratories). Mass spectrometric identification of proteins was performed as previously described⁵¹. Briefly, after SDS-PAGE, proteins were visualized by silver

staining and excised separately from gels, followed by the in-gel digestions with trypsin (Promega) in a buffer containing 50 mM ammonium bicarbonate (pH8.0) and 2 % acetonitrile overnight at 37° C. Molecular mass analyses of tryptic peptides were performed by matrix-assisted laser desorption/ionization time-of-flight mass spectrometry (MALDI-TOF/MS) using an Ultraflex TOF/TOF (Bruker Daltonics). Proteins were identified by comparison between the molecular weights determined by MALDI-TOF/MS and theoretical peptide masses from the proteins registered in NCBI. We subtracted the data corresponding to proteins in the control bands to identify the candidate TBP-2-specific binding proteins.

Supplementary Reference

51. Jensen, O.N., Podtelejnikov, A., & Mann, M. Delayed extraction improves specificity in database searches by matrix-assisted laser desorption/ionization peptide maps. *Rapid Commun Mass Spectrom* **10** 1371-1378 (1996).